BIOCHEMISTRY
including biophysical chemistry & molecular biology
Article

Biochemistry **2010,** *49,* 8177–8186 8177
DOI: 10.1021/bi1003487

Kinetic Analysis of 14-3-3-Inhibited *Arabidopsis thaliana* Nitrate Reductase[†]

Iris Lambeck,[‡] Jen-Chih Chi,[‡] Sabina Krizowski,[‡] Stefan Mueller,[§] Norbert Mehlmer,[∥,⊥] Markus Teige,[∥] Katrin Fischer,[‡] and Guenter Schwarz*[,‡]

[‡]*Institute of Biochemistry, Department of Chemistry, University of Cologne, 50674 Cologne, Germany,* [§]*Center for Molecular Medicine Cologne, Central Bioanalytics, University of Cologne, 50931 Cologne, Germany, and* [∥]*Department of Biochemistry and Cell Biology, MFPL, University of Vienna, 1030 Vienna, Austria.* [⊥]*Current address: Department of Biology I, Botany, Munich Center for Integrated Protein Science CiPSM, Ludwig-Maximilians-Universität München, D-82152 Planegg-Martinsried, Germany.*

Received March 8, 2010; Revised Manuscript Received August 5, 2010

ABSTRACT: Eukaryotic assimilatory nitrate reductase (NR) is a dimeric multidomain molybdo-heme-flavo protein that catalyzes the first and rate-limiting step in the nitrate assimilation of plants, algae, and fungi. Nitrate reduction takes place at the N-terminal molybdenum cofactor-containing domain. Reducing equivalents are derived from NADH, which reduce the C-terminal FAD domain followed by single-electron transfer steps via the middle heme domain to the molybdenum center. In plants, nitrate reduction is post-translationally inhibited by phosphorylation and subsequent binding of 14-3-3 protein to a conserved phosphoserine located in the surface-exposed hinge between the catalytic and heme domain. Here we investigated *Arabidopsis thaliana* NR activity upon phosphorylation and 14-3-3 binding by using a fully defined in vitro system with purified proteins. We demonstrate that among different calcium-dependent protein kinases (CPKs), CPK-17 efficiently phosphorylates Ser534 in NR. Out of eight purified *Arabidopsis* 14-3-3 proteins, isoforms ω, κ, and λ exhibited the strongest inhibition of NR. The kinetic parameters of noninhibited, phosphorylated NR (pNR) and pNR in a complex with 14-3-3 were investigated. An 18-fold reduction in k_{cat} and a decrease in the apparent $K_M^{nitrate}$ (from 280 to 141 μM) were observed upon binding of 14-3-3 to pNR, suggesting a noncompetitive inhibition with a preferential binding to the substrate-bound state of the enzyme. Recording partial activities of NR demonstrated that the transfer of electrons to the heme is not affected by 14-3-3 binding. The Ser534Ala variant of NR was not inhibited by 14-3-3 proteins. We propose that 14-3-3 binding to Ser534 blocks the transfer of electrons from heme to nitrate by arresting the domain movement via hinge 1.

Nitrogen assimilation in autotrophic eukaryotes is key for subsequent amino acid synthesis and nucleotide metabolism. Plants use ammonia, organic compounds, or nitrate as a suitable nitrogen source in soil, with the latter being the most important one (*1*). Specific transporters mediate the uptake of nitrate (*2*, *3*), which is either stored in the vacuole or directly converted to nitrite by the cytosolic enzyme nitrate reductase (NR).[1] Afterward, the reaction product nitrite, which is highly reactive, is transported into chloroplasts and reduced to ammonia via the [4Fe-4S] cluster- and siroheme-containing nitrite reductase (*4*).

As the last two reaction steps in nitrogen assimilation (nitrite reduction and glutamate synthesis) are restricted to chloroplasts, and reducing equivalents as well as nitrogen-accepting compounds are derived from photosynthetic processes, nitrogen assimilation and photosynthesis are closely coupled and highly regulated in a complex network on both the transcriptional and the post-translational level. For this purpose, NR presents a main target for regulatory intervention, because it catalyzes the first and rate-limiting step in nitrogen metabolism (*5*).

NR is a complex homodimeric enzyme in which each subunit possesses three cofactors bound to distinct and independently (except one) folded domains. The N-terminal domain harbors the molybdenum cofactor (Moco), which is the site of catalytic nitrate reduction and closely connected to the cofactor-free dimerization domain (*6*). The small central domain contains a b_5-type heme, and the C-terminal domain comprises the flavin adenine dinucleotide (FAD) cofactor as well as the NADH-binding site (*7*) (Figure 1). The central heme domain bridges both terminal domains via two protease-sensitive surface-exposed loops (hinge 1 and hinge 2).

While slow- and/or long-term changes in metabolism (e.g., availability of CO_2, nitrate, and light) are mainly mediated by transcriptional control of NR expression (*8*−*10*), sudden changes demand immediate control of enzyme activity on a post-translational level (*11*, *12*). It was previously shown that regulation of protein level overrules transcriptional control, as post-translational mechanisms could compensate for deregulated transcription of NR mRNA in plants (*13*).

Several studies demonstrated three modes of post-translational control of NR activity. (i) NR inhibition depends on a 14-3-3 protein that binds to a phosphorylated conserved serine residue (Ser534 in *Arabidopsis thaliana*) located in hinge 1 between the dimerization and heme domain (Figure 1) (*14*−*19*). (ii) Irreversible inhibition of the enzyme by degradation has been reported. However, it remains unclear whether phosphorylation of NR is

[†]This project has been funded by the Deutsche Forschungsgemeinschaft DFG (SFB 635 TP05 to G.S.) and by the Austrian FWF (Grants P16963-B12 and P19825-B12 to M.T.).

*To whom correspondence should be addressed. Phone: +49-221-470-6441. Fax: +49-221-470-5092. E-mail: gschwarz@uni-koeln.de.

[1]Abbreviations: CPK, calcium-dependent protein kinase; FAD, flavin adenine dinucleotide; Moco, molybdenum cofactor; NADH, reduced nicotinamide adenine dinucleotide; NR, nitrate reductase.

Published on Web 08/06/2010

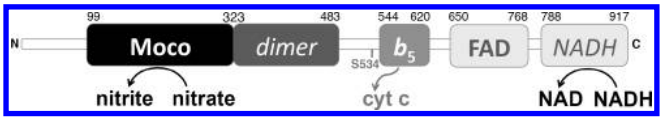

FIGURE 1: Schematic presentation of *Arabidopsis* nitrate reductase. Depicted are the cofactors (Moco, molybdenum cofactor; b_5, cytochrome b_5; FAD, flavin adenine dinucleotide), the dimerization domain (dimer), the NADH-binding domain (NADH), and the site of nitrate reduction and the artificial electron acceptor cytochrome *c* (cyt *c*).

involved in triggering protein degradation (*12*, *20*−*23*). (iii) Another suggested mechanism includes a yet not well described function of the nonconserved N-terminus of NR (*24*−*26*). Among these mechanisms, 14-3-3-mediated control of NR activity is considered to be the most important one for plants (*13*).

Phosphorylation of a serine residue (Arabidopsis Ser534) in NR hinge 1 is believed to be subject to different regulatory circuits, as members of both the calcium-dependent protein kinase family (CPK) (*27*, *28*) and the calcium-independent SNF1 resembling kinase family (SNRK1) have been shown to catalyze NR phosphorylation (*29*, *30*). Recent reports indicate a central role of the SNRK1 family in plant metabolism and energy balance (*31*) that would also involve NR regulation, but also for CPKs, a broad range of functions was assigned, including phosphorylation of NR (reviewed in ref *32*). The hinge 1 sequence of NR contains the canonical motif for both CPKs (*27*, *33*, *34*) and SNRK1s (*35*, *36*). Furthermore, it could be shown that CPKs and SNRK1 have overlapping substrate specificities (*27*, *29*, *37*, *38*), leaving open the question of the condition under which plant NR is phosphorylated by CPKs or SNRKs.

After phosphorylation, binding of a 14-3-3 protein imparts inhibition of phosphorylated NR (pNR). Until now, 13 expressed 14-3-3 isoforms in *Arabidopsis* that are highly similar on the primary and structural level have been identified (*39*, *40*). Several publications reported the affinity of various plant 14-3-3 proteins toward partially purified and phosphorylated NR or its synthetic peptides, showing that the affinities of the 14-3-3 proteins for pNR differ significantly, which is independent of the phylogenetic origin of the respective 14-3-3 protein. Also, affinities reported for different 14-3-3 proteins vary due to different experimental setups such as the use of partially purified NR or the use of different peptide-based interaction studies (*41*−*43*).

Here, we established a system for characterizing the molecular mechanism of post-translational regulation of *A. thaliana* NR with all involved proteins from *A. thaliana* being recombinantly expressed and purified to homogeneity. NR was initially characterized by steady-state kinetics and subjected to in vitro phosphorylation experiments. We identified CPK-17 as one of the kinases that is able to efficiently phosphorylate NR at Ser534. Finally, we determined binding affinities and inhibitory strengths of eight different 14-3-3 proteins from *A. thaliana*. Steady-state kinetics of NR and pNR showed similar kinetic parameters for both enzymes, while subsequent binding of 14-3-3 isoform ω, λ, or κ inhibited pNR activity most efficiently; on the other hand, a Ser534Ala variant of NR remained active in the presence of CPK-17 and 14-3-3. Furthermore, nitrite inhibition of holo-NR or pNR in a complex with 14-3-3 isoform ω remained similar. With the aid of artificial electron acceptors, we demonstrate that 14-3-3 binding inhibits the transfer of electrons from the heme domain to nitrate. Our finding of a mixed inhibition with preferential binding of 14-3-3 proteins to the substrate-bound state of the enzyme suggests an elegant mode of the nitrate-controlled strength of inhibition with an increased rate of release of 14-3-3 at low substrate concentrations.

EXPERIMENTAL PROCEDURES

Purification of Nitrate Reductase. *A. thaliana* nitrate reductase (NR) was purchased as affinity-purified protein (NECi, Lake Minden, MI). For further purification, anion exchange chromatography was performed with a SourceQ15 column (GE Healthcare, Uppsala, Sweden) using 50 mM Tris-HCl (pH 7.5) and 10 mM 2-mercaptoethanol as starting buffer A. With a gradient from 10 to 50% with buffer B (buffer A including 1 M NaCl) over 35 column volumes (CV), NR eluted at ∼30% buffer B. The NR-containing fractions were pooled and diluted with water to decrease the salt concentration below 100 mM. The protein was concentrated in a second anion exchange chromatography step using the same column and buffers but a steep gradient over 1−2 CV, yielding concentrations of up to 2 mg/mL. Prior to flash-freezing the protein in liquid nitrogen, we determined its concentration via absorbance at 413 nm using an extinction coefficient of 120 mM^{-1} cm^{-1} (*44*). The Moco/MPT content was detected via HPLC FormA anaylsis as described previously (*45*).

Cloning, Expression, and Purification of the Ser534Ala Mutant. Plasmid pKK001, which was kindly provided by N. Crawford (University of California, San Diego, CA), served as template for polymerase chain reaction (PCR). Specific primers were generated to introduce the site-directed mutagenesis of serine 534 to alanine and to insert 33 nucleotides between nucleotides 6 and 7 of the coding sequence, leading to an insertion of 11 residues (His_6Asp_4Lys) between residues 2 and 3 of NR. The amplified fragment was cloned into the *Eco*RI and *Kpn*I sites of pPICZB (Invitrogen, Darmstadt, Germany). For protein expression, the plasmid was transformed into *Pichia pastoris* strain KM71, and transformed cells were selected with 100 μg/mL zeocin on YPD agar plates for 2 days. The starter culture (200 mL of YPD with zeocin) in a baffled flask was inoculated with one colony and incubated overnight at 30 °C on a shaker. The 200 mL culture was split and used for inoculation of two larger cultures (2 × 500 mL of YPD in baffled flasks), which were grown for 30 h at 30 °C on a shaker. After the culture had been harvested, cells were resuspended in 2 × 500 mL of BMMH [containing 100 mM potassium phosphate (pH 6.0), 0.00004% biotin, 0.004% histidine, 1.34% Yeast Nitrogen Base, 250 μM Na_2MoO_4, 10 μM $FeCl_2$, and 1% methanol] for induction. The expression cultures were incubated on the shaker for 12 h at 30 °C, harvested, and resuspended in lysis buffer containing 20 mM Tris-HCl (pH 7.5), 300 mM NaCl, 10% glucose, 50 mM imidazole, and 15 mM glutathione. Cell extraction was perfomed using a cell disruptor (Constant Systems Ltd.) and sonication, followed by centrifugation. The supernatant was supplemented with a mix of 25 mM arginine and 25 mM glutamine (adjusted to pH 7.5) before application on a Ni-NTA matrix (GE Healthcare). After unbound proteins had been washed out, the protein was eluted with lysis buffer containing 500 mM imidazole. The protein was frozen in liquid nitrogen at a concentration of 50 μg/mL. To demonstrate successful purification of NR-Ser534Ala, an immunoblot was performed using a polyclonal anti-NRMo domain antibody followed by an alkaline phosphatase-coupled secondary antibody.

Cloning, Expression, and Purification of the Kinases. CPKs CPK-2 (At3g10660), CPK-3 (At4g23650), CPK-16

(At2g17890), CPK-17 (At5g12180), CPK-24 (At2g31500), and CPK-29 (At1g76040) were amplified via PCR and cloned in frame as *Bam*HI/*Not*I fragments into GST fusion expression plasmid pGEX4-T1 (GE Healthcare). The expression plasmid for the loss-of-function mutant of CPK-3-LOF was made by site-directed mutagenesis of arginine 107 to lysine with the site-directed mutagenesis QuickChange kit (Stratagene, La Jolla, CA) using expression plasmid pGEX4T1-CPK-3 as a template.

Escherichia coli strain BL21-CodonPlus (Stratagene) was transformed with each expression construct and used to inoculate LB supplemented with 100 μg/mL ampicillin. Overnight cultures were diluted to an OD_{600} of ≈0.2. After the cultures had grown at 37 °C to an OD_{600} of ≈0.6, protein expression was induced with 1 mM IPTG and the cells were harvested after 4 h at 28 °C. The cells were resuspended in PBS and lysed using a cell disruptor (Constant Systems Ltd., Daventry, U.K.) followed by sonication. The crude extract was centrifuged, and the supernatant was applied on a glutathione Sepharose 4 fast flow matrix (GE Healthcare). Elution was performed with a buffer containing 50 mM Tris-acetate (pH 8.0) and 10 mM glutathione. The protein was aliquoted and flash-frozen in liquid nitrogen.

Phosphorylation of NR. Kinase assays were performed by incubation of ~1 μg of recombinant protein kinase, 5 μg of NR, and 2 μCi of [γ-^{32}P]ATP in kinase buffer [20 mM HEPES (pH 7.6), 1 mM DTT, and 5 mM $MgCl_2$] in the presence of 100 μM Ca^{2+} or 1 mM EGTA. After incubation at room temperature for 30 min, addition of SDS−PAGE loading buffer terminated the reaction. The samples were analyzed by SDS−PAGE. The incorporation of radioactivity was measured by exposing the dry gel overnight on a storage phosphor screen that was scanned in a GE Healthcare Typhoon 8600 Variable Mode Imager. As CPK-17 produced the strongest phosphorylation signal of NR, all further phosphorylation experiments were conducted using CPK-17.

For large-scale protein expression, the plasmid containing CPK-17 was transformed into *E. coli* BL21-CodonPlus (DE3)-RIPL cells (Stratagene). After the culture had grown at 37 °C to an OD_{600} of ≈0.6, protein expression was induced with 100 μM IPTG and the cells were harvested after 4 h at 25 °C. The cells were resuspended in PBS and lysed using a cell disruptor (Constant Systems Ltd.) followed by sonication. The crude extract was centrifuged, and the supernatant was applied on a glutathione Sepharose 4 fast flow matrix (GE Healthcare). Elution was performed with a buffer containing 50 mM Tris-acetate (pH 8.0) and 10 mM glutathione. Afterward, CPK-17 was buffer-exchanged into assay buffer [50 mM Bis-Tris-acetic acid (pH 7.0), 50 mM KCl, 5 mM magnesium acetate, and 1 mM $CaCl_2$]. The protein was aliquoted and flash-frozen in liquid nitrogen.

Preparative phosphorylation of NR for kinetic studies was conducted with 2−8 μM NR and 0.2−0.8 μM CPK-17 in assay buffer containing 0.4 mM ATP. During the 1 h incubation, the reaction setup was concentrated using centripreps (Millipore, Billerica, MA) to enhance the phosphorylation efficiency in the case of low binding affinities. In the first assays, pNR was separated from the kinase by running a Superdex 200 5/150 GL gel filtration column (GE Healthcare) using 100 mM Tris-HCl (pH 7.5), 300 mM NaCl, 5 mM $MgCl_2$, 1 mM $CaCl_2$, and 1 mM 2-mercaptoethanol as the running buffer. As no difference was found in the kinetic behavior of pNR in the presence or absence of kinase and ATP (data not shown), the gel filtration step was left out to retain maximum amounts of pNR for the kinetic experiments.

Phosphorylation Studies of NR-Ser534Ala. Wild-type NR or NR-Ser534Ala (240 ng of either) was phosphorylated with 24 ng of CPK-17 using [γ-^{32}P]ATP as described for preparative phosphorylation of wild-type NR. The phosphorylation was stopped by addition of SDS gel loading buffer; proteins were separated via 10% SDS−PAGE, and incorporation of radioactivity was assessed via exposure of the dry gel for 15 min to a radiographic film. After the gel had developed and dried, the marker sizes were defined by overlaying the dry gel with the film.

Mass Spectrometry. Prior to digestion, proteins were precipitated with acetone. Briefly, 3 volumes of ice-cold acetone was added to the prechilled samples, and proteins were allowed to precipitate for 1 h at −20 °C. The samples were centrifuged for 10 min at 14000*g* and 4 °C in a benchtop centrifuge. The supernatants were removed, and the pellets were washed once with prechilled acetone. Air-dried pellets were resuspended in 8 M urea, 50 mM Tris-HCl (pH 8.0), and 10 mM DTT, and proteins were denatured and reduced by incubation at 60 °C for 45 min. To S-alkylate reduced cysteine residues, iodoacetamide was added to a final concentration of 25 mM, and the reaction was allowed to proceed for 30 min in the dark. Prior to digestion, the samples were diluted 1:4 in 50 mM Tris-HCl (pH 8.0), and trypsin (sequencing grade, Promega) was added to a final concentration of 12.5 ng/μL. Proteins were digested at 37 °C overnight. After addition of 0.1 volume of 1% TFA, the digest was loaded onto a PepClean C18 spin column (Pierce) equilibrated in 0.1% TFA. The column was washed with 0.1% TFA, and peptides were eluted with 80% acetonitrile in 0.1% TFA. Phosphopeptides were enriched on titanium dioxide-coated magnetic beads using the PhosTrap phosphopeptide enrichment kit (Perkin-Elmer) according to the manufacturer's instructions.

For MALDI-TOF MS of protein digests, 1.0 μL of the extracted total peptides or TiO_2-enriched phosphopeptides was mixed with 1.2 μL of 2.5 mg/mL 2,5-dihydroxybenzoic acid in a 0.1% TFA/acetonitrile (2:1) mixture and spotted onto a 800 μm anchor target (Bruker Daltonics, Bremen, Germany). Positive ion spectra were recorded on a Reflex IV MALDI-TOF mass spectrometer (Bruker Daltonics) in the reflectron mode. A peptide calibration standard (Bruker Daltonics) was used for external calibration of the mass range from m/z 1046 to 3147. The FlexAnalysis postanalysis software was used for optional internal recalibration on trypsin autolysis peaks and the generation of peaklists. Biotools 3.0 (Bruker Daltonics) was used for the interpretation of mass spectra with regard to the expected sequence of nitrate reductase.

For liquid chromatography with tandem mass spectroscopy (LC−MS/MS) of protein digests, LC−MS data were acquired on a Q-TofII quadrupole-TOF mass spectrometer (Micromass, Manchester, U.K.) equipped with a Z spray source. Samples were introduced with an Ultimate Nano-LC system (LC Packings, Amsterdam, The Netherlands) equipped with a Famos autosampler and a Switchos column switching module. The column setup comprises a 0.3 mm × 1 mm trapping column and a 0.075 mm × 150 mm analytical column, both packed with 3 μm Atlantis dC18 (Waters). Enriched phosphopeptides were dried down in a speed vac and were solubilized in 0.1% TFA. A total of 10 μL was injected onto the trap column and desalted for 1 min with 0.1% TFA and a flow rate of 10 μL/min. The 10-port valve switched the trap column into the analytical flow path, and peptides were eluted onto the analytical column by using a gradient of 2% acetonitrile (ACN) in 0.1% FA to 40% ACN in 0.1% FA over 65 min and a column flow rate of ca. 200 nL/min,

resulting from a 1:1000 split of the 200 μL/min flow delivered by the pump. The electrospray ionization (ESI) interface comprised an uncoated 10 μm (inside diameter) PicoTip spray emitter (New Objective) linked to the HPLC flow path using a 7 μL dead volume stainless steel union mounted onto the PicoTip holder assembly (New Objective). Stable nanospray was established by the application of 1.7−2.4 kV to the stainless steel union. The datum-dependent acquisition of MS and tandem MS (MS/MS) spectra was controlled by Masslynx version 4.0. Survey scans of 1.4 s covered the range from *m*/*z* 400 to 1400. Doubly and triply charged ions rising above a given threshold were selected for MS/MS experiments. In MS/MS mode, the mass range from *m*/*z* 40 to 1400 was scanned in 1.4 s, and four scans were summed for each experiment. Micromass-formated peaklists were generated from the raw data by using the Proteinlynx software module.

Phosphopeptides were identified by searching a custom database containing the expected nitrate reductase sequence using a local installation of MASCOT version 1.9. Searches were submitted in MASCOT with the following parameter settings: enzyme, "trypsin"; species, "plant"; fixed modifications, "carbamidomethyl"; optional modifications, "methionine oxidation" and "serine", "threonine" or "tyrosine phosphorylation"; missed cleavages, "1". The mass tolerance is set to 0.3 Da for peptide and fragment ions. All spectra that lead to phosphopeptide identification were evaluated and annotated manually.

Cloning, Expression, and Purification of 14-3-3 Protein Isoforms. The cDNAs of 14-3-3 isoforms χ (At4g09000.1), ω (At1g78300.1), ψ (At5g38480.1), υ (At5g16050.1), λ (At5g10450.2), ν (At3g02520.1), κ (At5g65430.1), and ε (At1g22300.3) were amplified from an *A. thaliana* cDNA library [(i) from 3-week-old green plants, (ii) from cell suspension cells, (iii) from young green plants, (iv) from flowering plants, or (v) from flowers and roots of green plants] and cloned into the *Nde*I and *Bam*HI sites of the pET15b vector (Novagen), resulting in the expression of proteins with an N-terminal His_6 tag. For protein expression, the plasmids were transformed into *E. coli* BL21-CodonPlus (DE3)-RIPL cells. After the induction of protein expression at an OD_{600} of ∼0.6 with 100 μM IPTG, the cultures were harvested after overnight incubation at 20 °C (isoforms χ, ψ, υ, and ε), 25 °C (ω and κ), 30 °C (λ), or 37 °C (ν). All 14-3-3 proteins were purified in the same way, starting with resuspension of the cell pellet in lysis buffer [100 mM potassium phosphate, 300 mM sodium chloride, and 20 mM imidazole (pH 7.5)]. Cell extract preparation was performed as described above, and the crude extract supernatant was then applied onto a Ni-NTA matrix (Qiagen, Hilden, Germany). The matrix was washed with lysis buffer, and then the bound proteins were eluted using lysis buffer containing 500 mM imidazole. Dialysis or size exclusion chromatography using a Superdex 200 26/60 pg column (GE Healthcare) was conducted to buffer-exchange the proteins into assay buffer. The proteins were aliquoted, flash-frozen in liquid nitrogen, and stored at −80 °C at concentrations between 20 and 50 mg/mL. Native folding of all 14-3-3 proteins was approved by recording far-UV circular dichroism spectra using a JASCO model J-715 instrument (JASCO, Gross-Umstadt, Germany). Protein samples were buffer-exchanged via PD10 columns (GE Healthcare) into 10 mM potassium phosphate (pH 7.4) and adjusted to a concentration of 2.5−4.9 μM. All measurements were performed at 20 °C in a 1 mm path-length cuvette. For each measurement, 20 spectra were recorded at a scan speed of 100 nm/min with a step resolution of 0.1 nm. The spectra were corrected for a protein-free spectrum obtained under identical conditions. Noise reduction was applied according to the JASCO software, and the obtained raw data were converted into mean residue ellipticity.

Kinetics. All enzyme assays were performed at room temperature in assay buffer. The reactions were followed photometrically using an ELISA reader EL808 IU (BioTek, Winooski, VT), and all data are mean values of at least triplicate measurements. For nitrate-dependent reduction of NADH (NADH assay), 42 nM NR/pNR and 220 μM NADH were mixed with up to 2 μM 14-3-3 protein where appropriate and preincubated for 5 min at room temperature. The reaction was started with 10−1000 μM potassium nitrate, and the oxidation of NADH was recorded by following the decrease in absorbance at 340 nm. As the presence or absence of the kinase did not yield differences in the kinetic experiments, pNR was used for subsequent studies without further purification. For the cytochrome *c* assay, 0.6 nM NR/pNR, 100 μM cytochrome *c*, and up to 2 μM 14-3-3 were preincubated for 5 min at room temperature. The NADH-dependent reduction of cytochrome *c*, which accepts electrons from the heme domain, was started with 0−50 μM NADH, and the increase in A_{550} was recorded, indicating reduction of cytochrome *c*.

Comparative inhibition studies of NR-Ser534Ala with 14-3-3 proteins were conducted as described for the wild type using 40 nM protein for phosphorylation followed by incubation with each 14-3-3 at 2 μM or buffer as a control. The activities were measured as described above using 2 mM nitrate as the substrate.

Nitrite Inhibition. The inhibitory effect of nitrite was tested in the NADH nitrate assay using 50 nM NR or pNR with 14-3-3 isoform ω, 2 mM nitrate, and 0−60 mM sodium nitrite. The inhibition was calculated on the basis of the noninhibited enyzme's activity.

RESULTS

Characterization of Arabidopsis NR. Partially purified His-tagged *Arabidopsis* NR was purchased from NECi. The protein had been expressed in *Pichia pastoris* and was enriched via Ni affinity chromatography. Further purification was achieved by anion exchange chromatography (Figure 2A), yielding highly pure enzyme with only minor contaminating protein bands (Figure 2A, inset). As seen in the chromatogram, the main NR-containing peak shows a strong absorption at 413 nm, indicating the presence of the heme cofactor. Attempts to concentrate the protein by ultrafiltration resulted in strong precipitation. Therefore, the protein was concentrated via anion exchange chromatography using a short and steep salt gradient resulting in protein concentrations of up to 2 mg/mL.

The NR concentration was determined via the absorbance at 413 nm, using an extinction coefficient of 120 mM^{-1} cm^{-1} (*44*) as a measure of the heme saturation of the enzyme (Figure 2B). The oxidized spectrum of NR depicts an additional major absorption band at 260 nm and a shoulder at 460 nm that originate from bound FAD (*44*). Upon reduction with excess NADH, the typical Soret band of the heme cofactor shifted from 413 to 424 nm, the FAD-derived shoulder (460 nm) underwent a reduction in absorption, and two additional peaks at 528 and 557 nm developed. The presence of the third cofactor, Moco, could not be monitored by UV−vis spectroscopy, because its two typical but weak signals at 350 and 480 nm were masked in both the oxidized and reduced spectra by the heme and FAD signals. The Moco content of NR was determined by HPLC analysis of

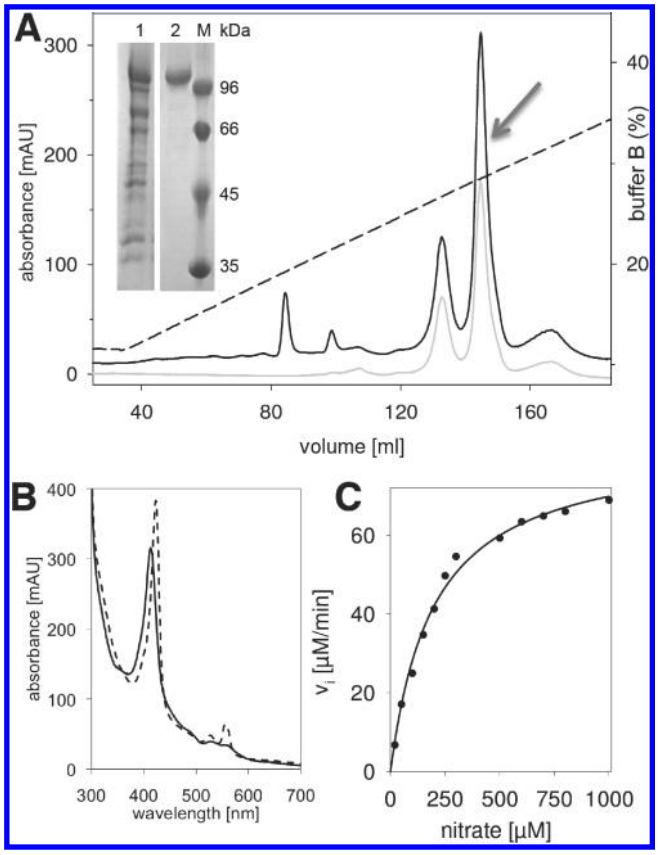

FIGURE 2: Purification and characterization of NR. (A) Anion exchange chromatography of NR. Shown are the absorption at 280 nm (solid black line) and 413 nm (solid gray line) and the conductivity (dashed line). The NR-containing peak marked with an arrow was collected and concentrated. The 10% SDS−PAGE in the inset depicts NR before (lane 1) and after (lane 2) purification by anion exchange chromatography (M, marker). (B) The UV−vis spectra of purified NR under oxidizing conditions (solid line) and after reduction with 10 μM NADH (dashed line) demonstrate the typical Soret band shifts and the additional peaks at 527 and 557 nm that develop upon reduction. (C) Michaelis−Menten kinetics of NR (40 nM, based on Moco content) using the physiological substrates nitrate and NADH results in a $K_M^{nitrate}$ of 197 μM and a k_{cat} of 33 s^{-1}. The Michaelis−Menten curve was fitted using SigmaPlot.

its oxidation product FormA-dephospho, demonstrating 60% cofactor saturation (data not shown).

Steady-state kinetics using the physiological substrates nitrate and NADH determined for nitrate a $K_M^{nitrate}$ of 197 ± 15 μM and a $k_{cat}^{nitrate}$ of 33 ± 0.8 s^{-1}, with the latter being calculated on the basis of the Moco content of the protein (Figure 2C). On the basis of the heme content, this $k_{cat}^{nitrate}$ corresponds to 20 s^{-1}. The half-life of purified and active NR at 4 °C under aerobic conditions was determined to be 3.5 days (data not shown), confirming the high purity and stability of our preparation.

Phosphorylation of NR. A variety of plant protein kinases are implicated in NR phosphorylation, leading to 14-3-3-mediated inhibition of the enzyme. These kinases were allocated either to members of the SNF1-related protein kinase family (*29*) or to members of the calcium-dependent protein kinase family (CPK) (*27*). As the sequence of NR encompassing the phosphorylated Ser534 complies with the canonical recognition motif of CPKs, we have chosen six different enzymes (CPK-2, -3, -16, -17, -24, and -29) to identify a kinase with high in vitro phosphorylation activity toward NR using [γ-^{32}P]ATP as a substrate. SDS−PAGE and subsequent autoradiograph analysis of

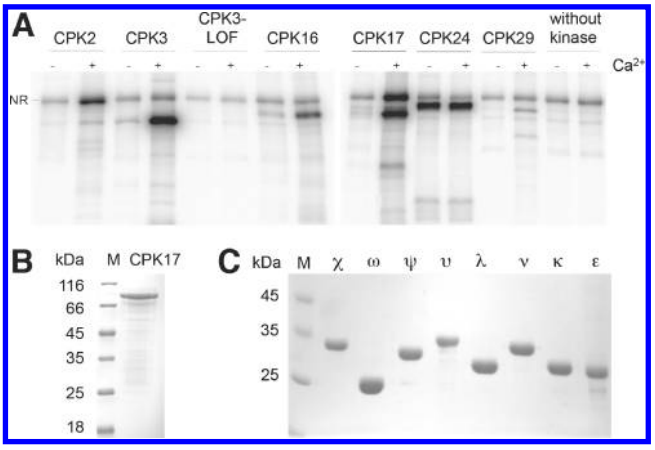

FIGURE 3: Phosphorylation of NR and purification of CPK-17 and 14-3-3 proteins. (A) NR phosphorylation by different CPKs (CPK-2, -3, -16, -17, -24, and -29) was demonstrated in the presence or absence of 100 μM calcium using radioactively labeled ATP. As a negative control, a loss-of-function variant of CPK-3 (CPK3-LOF) or no kinase (without kinase) was added to the assay. The reaction mixtures were separated via 10% SDS−PAGE, and successful phosphorylation was detected by autoradiography. (B) SDS−PAGE (12%) of affinity-purified (via glutathione Sepharose) and buffer-exchanged CPK-17. (C) SDS−PAGE (15%) of the investigated His-tagged 14-3-3 isoforms (χ, ω, ψ, υ, λ, ν, κ, and ε) after affinity purification (Ni-NTA) and buffer exchange.

^{32}P-labeled NR demonstrated calcium-dependent NR phosphorylation by CPK-17 and CPK-2, while others such as CPK-16, -24, and -29 exhibited virtually no activity; bands are comparable to the lanes in which an inactive (loss of function) kinase has been used (Figure 3A). Therefore, CPK-17 was recombinantly expressed as a GST-tagged fusion protein on a large scale and purified to homogeneity (Figure 3B).

For the following functional studies, NR was incubated with CPK-17 and 10 mM ATP in assay buffer, and the phosphorylated NR (pNR) was separated from the kinase by size exclusion chromatography. Successful and efficient phosphorylation of Ser534 was confirmed by mass spectrometry (Figures 1 and 2 of the Supporting Information). As expected, a tryptic peptide with a mass of 1363.6 Da showed the strongest signal in the TiO_2-enriched fraction of peptides and was subsequently confirmed to carry a single phopshorylation at Ser534 (Figure 2 of the Supporting Information). As a note, less intense signals of other peptides were found upon TiO_2 enrichment; some peptides were clearly nonphosphorylated, while others were partially phosphorylated but could not further be analyzed by MS/MS because of their low abundance (Figure 1 of the Supporting Information). Two peptides were found to be phosphorylated substoichiometrically; one was a second phosphorylation at the peptide mentioned above carrying pSer534, while the other phosphorylation was found on Ser34. In summary, we could confirm Ser534 as a major phosphorylation site in NR.

Inhibition by 14-3-3 Protein Binding. So far, 13 different 14-3-3 proteins have been identified in *Arabidopsis*, which can be assigned to four groups (A−D) on the basis of their phylogeny (*46*). To study 14-3-3-mediated inhibition of pNR, we PCR-cloned and purified eight (χ, ω, ψ, υ, λ, ν, κ, and ε) of these 14-3-3 proteins for which expression in *Arabidopsis* had been demonstrated previously (*47*, *48*). Different approaches to amplifying the five remaining isoforms (ι, μ, φ, o, and π) from various cDNA libraries failed; hence, we restricted our studies to the eight available homologues. All 14-3-3 proteins were expressed as

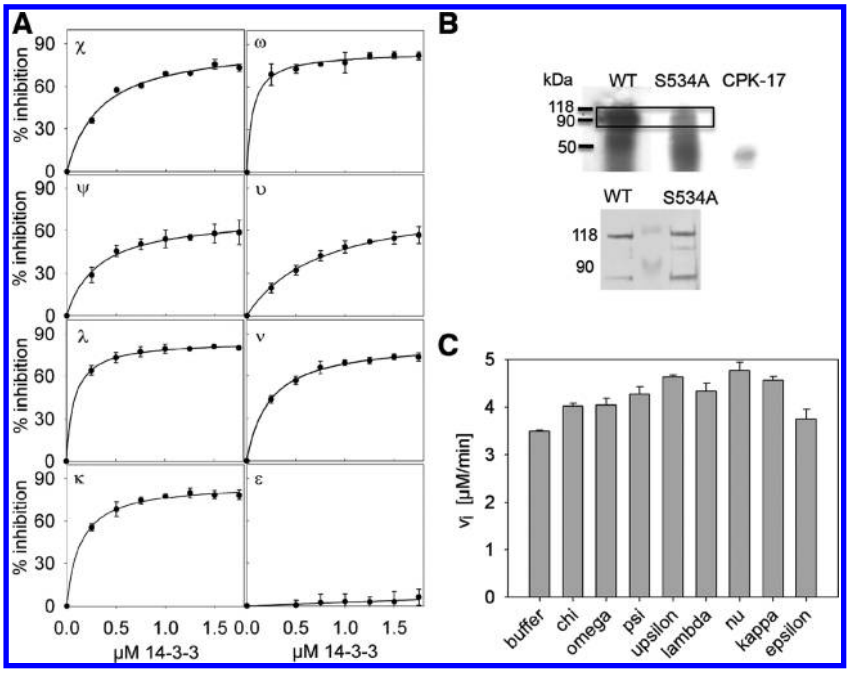

FIGURE 4: Activity of pNR and pNR-Ser534Ala in the presence of 14-3-3 proteins. (A) Nitrate-NADH assays were performed under substrate saturating conditions (220 μM NADH and 1 mM nitrate) using pNR (42 nM). Prior to the assay, pNR was incubated with varying concentrations of each 14-3-3. The measured activities were plotted as the relative inhibition by setting the pNR activity without 14-3-3 to 0% inhibition. The graphs were generated and fitted using SigmaPlot. (B) Radiograph of wild-type NR and the Ser534Ala mutant (top) and anti-NRMo immunoblot of the corresponding proteins (bottom). The radiograph demonstrates much stronger phosphorylation of the wild type with ATP (black frame), whereas CPK-17 alone gives no signal around 100 kDa. The immunoblot of wild-type NR and the Ser534Ala mutant was performed using an anti-NRMo antibody and demonstrates equal loading. (C) Inhibition assays with the NR-Ser534Ala mutant (40 nM) after phosphorylation treatment and incubation with each 14-3-3 (2 μM) or buffer as a control. No decrease in activity can be monitored.

His-tagged proteins in *E. coli* and purified to homogeneity (Figure 3C). All proteins were highly soluble and showed a similar CD spectrum confirming their conformational integrity (Figure 3 of the Supporting Information).

To test the inhibition efficiency of purified 14-3-3 proteins, pNR was incubated for 5 min with each 14-3-3 protein prior to the assay of the NADH-dependent nitrate reduction. A clear dose-dependent inhibition of pNR activity was observed (Figure 4A) for all 14-3-3 proteins except for 14-3-3 isoform ε, the only available member of group D. Nonetheless, the binding affinity and inhibition strength of the other seven 14-3-3 proteins varied significantly, as summarized in Table 1, and no specificity based on the phylogenetic groups was observed. On the basis of the inhibition strength of 84% and the K_i of 60 nM, 14-3-3 isoform ω was found to be the strongest inhibitor of pNR, closely followed by 14-3-3 isoform λ. The fact that even with 14-3-3 isoform ω only 84% total inhibition could be achieved points to an incomplete phosphorylation of NR. Control experiments demonstrated that neither pNR in the absence of 14-3-3 proteins nor incubation of 14-3-3 with nonphosphorylated NR resulted in any significant impairment of NADH-dependent nitrate reduction (data not shown), which is consistent with previous findings using partially purified NR (*49*).

In light of the fact that we found additional phosphorylation sites in NR (Figure 1 of the Supporting Information), we also generated a Ser534Ala variant and investigated the phosphorylation of this protein with respect to wild-type NR. We observed a strong reduction in the level of phosphorylation when subjecting similar amounts of wild-type NR and NR-Ser534Ala to the in vitro phosphorylation assay described above using [γ-^{32}P]ATP (Figure 4B). However, none of the 14-3-3 proteins investigated here was able to inhibit the CPK17-treated Ser534Ala variant, suggesting that phosphorylation of Ser534 is crucial for mediating 14-3-3 inhibition of NR (Figure 4C).

Table 1: Binding Affinities (K_i) and Inhibition Strengths (I_{max}) of 14-3-3 Proteins with pNR[a]

	χ	ω	ψ	υ	λ	ν	κ	ε
K_i (nM)	340	60	310	760	80	230	140	–
I_{max} (%)	90	84	70	83	85	85	87	–

[a]Maximal inhibition (I_{max}) and the 14-3-3 protein concentration that gives half-maximal inhibition (K_i) were calculated from the inhibition titrations shown in Figure 3 using SigmaPlot.

Steady-State Kinetics. To define the part of the enzyme that is inhibited by 14-3-3 binding, steady-state kinetics were performed with different electron acceptors to monitor selectively electron transfer within the distinct NR domains. The physiological substrates NADH and nitrate were used to analyze the electron transfer involving all three NR cofactors, whereas using cytochrome *c* instead of nitrate provides information about the first substeps of the reaction, the transfer of electrons from NADH via FAD to the heme (Figure 1) excluding the regeneration of Moco and the reduction of nitrate. The NADH−nitrate assay clearly demonstrated that 14-3-3 isoform ω is a potent inhibitor of NR (Figure 5A), and the presence of 14-3-3 isoform ω reduced the apparent k_{cat} from 33 to 1.8 s^{-1}. Although the k_{cat} for pNR is comparable to that of unmodified NR, the K_M for nitrate was slightly increased. The fact that $K_M^{nitrate}$ decreased to 141 ± 25 μM for the 14-3-3-inhibited enzyme suggests a noncompetitive mode of action.

In contrast, the NADH−cytochrome *c* assay did not show any impact of 14-3-3 isoform ω on the electron transfer (Figure 5B),

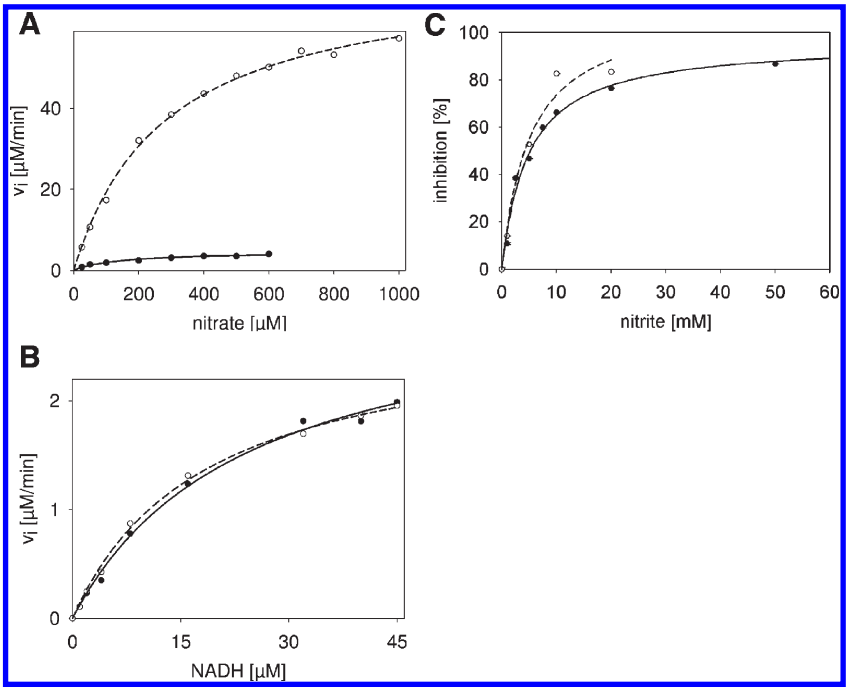

FIGURE 5: Steady-state kinetics of NR and pNR with and without 14-3-3 isoform ω. (A) Michaelis−Menten kinetics of pNR (42 nM) using 220 μM NADH and 0−1 mM nitrate in the absence (○, dashed line) or presence of 2 μM 14-3-3 isoform ω (●, solid line) showed clear inhibition of the enzyme. (B) Michaelis−Menten kinetics of pNR (0.6 nM) using 100 μM cytochrome *c* and 0−45 μM NADH in the absence (○, dashed line) or presence of 2 μM 14-3-3 isoform ω (●, solid line) did not indicate 14-3-3-mediated inhibition of the electron transfer steps from NADH to heme and cytchrome *c*. Note that, because of the higher extinction coefficient of cytochrome *c*, much less enzyme was used compared to the amount in the reaction shown in panal A (NADH-dependent nitrate reduction), and therefore, the velocities differ in the settings. (C) Titration of NR (●, solid line) or the pNR−14-3-3 isoform ω complex (○, dashed line) with increasing concentrations of nitrite under substrate saturation (2 mM nitrate). Similar $K_i^{nitrite}$ values of 4.8 ± 0.5 mM (NR) and 5.0 ± 1.5 mM (complex) indicate that the inhibitiory effect of nitrite is not altered upon 14-3-3 binding.

with both k_{cat} (50 s^{-1}) and K_M^{NADH} remaining unaltered (23 μM with and 18 μM without 14-3-3 isoform ω). These findings indicate that NADH oxidation and electron transfer up to the heme domain are not affected at all, whereas 14-3-3 binding seems to inhibit the second part of the reaction. To rule out the possibility that product release is affected by 14-3-3, we investigated nitrite inhibition of nonphosphorylated NR and pNR in complex with 14-3-3 isoform ω. We found in both cases similar K_i values of 4.8 ± 0.5 and 5.0 ± 1.5 mM, respectively (Figure 5C). Therefore, we conclude that 14-3-3 proteins most likely inhibit the transfer of electrons from heme via Moco to nitrate.

DISCUSSSION

We were able to purify recombinantly expressed plant NR to homogeneity. On the basis of the heme content of NR, a k_{cat} of 20 s^{-1} was recorded in this work, which is lower than that reported earlier by Skipper and co-workers also using recombinantly expressed *Arabidopsis* NR (*44*, *50*), where a k_{cat} of 42 ± 6 s^{-1} was reported (based on the heme content). However, when taking into account the Moco saturation, Skipper and co-workers described a k_{cat} of 210 s^{-1}, whereas the NR in our work would give a k_{cat} of only 33 s^{-1} based on Moco content. The question of whether the different turnover numbers, which most likely originate from different cofactor saturations, are sufficiently reliable to serve as a reference remains open. Similar deviations are observed in the K_M values obtained here or from previous publications: a review article (*51*) finds that $K_M^{nitrate}$ is in the range of 8−100 μM for NR from *Chlorella* (*52*), *Pichia* (*53*), and *Arabidopsis* (*44*). While Skipper et al. determined a $K_M^{nitrate}$ of 90 ± 20 μM, we obtained a value of 197 ± 15 μM. This deviation can be explained by the presence of 50 mM KCl in the assay buffer, which we found to increase protein stability and solubility dramatically (data not shown); thus, it was not omitted from the buffer. It has been shown previously for NR (*54*) as well as the homologous sulfite oxidase (*55*) that anions including chloride compete for substrate binding. With regard to the K_M for NADH, our measured K_M^{NADH} of 18 μM localizes well within the range of published K_M^{NADH} values for different plant NRs, being between 0.7 and 22 μM (*44*, *56*, *57*).

With a pure and stable NR in hand, we were able to establish a fully characterized in vitro system for analyzing the impact of phosphorylation and 14-3-3 binding on NR activity. As the phosphorylation sequence of NR complies with a canonical recognition motif of CPKs, we focused our work on those kinases to find a kinase for in vitro phosphorylation of *Arabidopsis* NR. We identified CPK-17 as a kinase that efficiently phosphorylates NR at Ser534. Although mass spectrometry also spotted other phosphorylated sites (with low stoichiometry), pSer534 had by far the strongest signal, and most importantly, a Ser534Ala variant was not inhibited by any of the eight 14-3-3 isoforms. In our experiments with wild-type pNR, all tested 14-3-3 isoforms except for 14-3-3 isoform ε were strong inhibitors, reaching maximal inhibition levels of 70−90%, whereas the affinities of 14-3-3 proteins for pNR (determined as K_i) varied by more than 1 order of magnitude from 60 to 760 nM. In former studies, the maximal inhibition levels were around 70% (*58*), meaning that in our work more NR was present in its phosphorylated state and/or other factors negatively impacting NR phosphorylation and/or 14-3-3 binding were excluded from this system. The observed residual activity with even the strongest 14-3-3 binding proteins might reflect an incomplete phosphorylation of Ser534.

The different inhibitions of 14-3-3 proteins point to the fact that not all 14-3-3 proteins bind pNR with the same affinity. On the basis of the ratio of inhibition strength to binding affinity, the analyzed 14-3-3 proteins can be classified as follows: $\omega > \lambda > \kappa > \nu > \gamma > \psi > \upsilon \gg \varepsilon$ (isoform ε having no inhibitory strength at all and isoform λ being almost as potent as isoform ω). This order is roughly in agreement with earlier publications (*42*, *59*) but seems to be in contrast to a recent report by Manak and Ferl (*43*). They analyzed the binding of 14-3-3 to a synthetic phosphopeptide of *Arabidopsis* NR Ser534 as a function of the concentration of either magnesium or calcium using surface plasmon resonance. Their finding with 14-3-3 isoform ε is one of the strongest ligands in the presence of high concentrations of either cation cannot be confirmed by our work. However, our experimental setup clearly differs from previous approaches. First, we used NR inhibition as direct readout for 14-3-3 specificity, which does not exclude binding of 14-3-3 protein to pNR as such. It is conceivable that 14-3-3 isoform ε binding to Ser534 is not sufficient for pNR inhibition because of other yet to be identified mechanisms contributing to the block in electron transfer toward the substrate identified here. Therefore, 14-3-3 isoform ε could serve also a regulatory role by blocking the binding site for other 14-3-3 isoforms. Second, the sequence of 14-3-3 sequence ε used by Manak and Ferl (*43*)(cDNA accession number U36446) corresponds to splice variant 1 (At1g22300.1), whereas we worked with splice variant 3 (At1g22300.3) that differs in 15 residues at the end of the protein (see Figure 4 of the Supporting Information). Third, all inhibition experiments were performed in the presence of both calcium and magnesium ions at physiological concentrations, and the use of a full-length enzyme instead of small synthetic peptides ensures a native environment for 14-3-3 binding, which altogether could explain the observed differences.

One explanation for the different affinities of 14-3-3 for pNR might be their organel- and development-dependent expression in the plant. It was shown that 14-3-3 isoform ω has been found exclusively in the cytosol, whereas isoforms μ, ε, ν, and υ have also been found in the stroma of chloroplasts (*60*). Three of these isoforms (ν, υ, and ε) have been analyzed in this work, showing significantly weaker binding to pNR, in contrast to the strictly cytosolically localized 14-3-3 isoform ω or the ubiquitously found 14-3-3 isoforms λ and κ (reviewed in ref *61*). In addition, a recent proteomic study using *Arabidopsis* 14-3-3 isoform ω resulted in the identification of ~300 client proteins of which NR was identified several times (*62*). Other 14-3-3 proteins are only induced upon stress signals, e.g., 14-3-3 isoform π, which is expressed only under conditions of permanent light exposure (*48*). Moreover, 14-3-3 isoform ω has also been identified in a proteomics approach that aimed to identify targets and interaction partners of CPK-3 (*63*).

Despite the isoform differences in inhibition efficacy, we were able to determine for the first time the type of NR inhibition by 14-3-3 proteins: an apparent increase in substrate binding affinity (K_M decreases from 197 to 141 μM) together with a dramatically decreased turnover number clearly points to a mixed type of inhibition. Because of this increase in affinity, a preference of inhibitor binding toward the substrate-bound state of the enzyme can be deduced. When using the artificial electron acceptor cytochrome *c* instead of nitrate, we could narrow the point of action where 14-3-3 binding intervenes during the catalytic cycle of NR. The observation that the transfer of electrons from the physiological donor NADH via FAD to heme is not impaired by 14-3-3 binding clearly demonstrates that 14-3-3 proteins act further downstream. Together with the finding that product release is not affected by 14-3-3 proteins (nonaltered nitrite inhibition), we can conclude that 14-3-3 proteins inhibit the transfer of electrons from the heme domain to nitrate. However, our experimental setup cannot distinguish whether the transfer of electrons from the heme cofactor to Moco is affected or the substrate reduction at the active site is impaired. The observation that the linker between Moco and the heme domain is surface-exposed and flexible leads to the hypothesis that 14-3-3 binding arrests the conformational freedom of the linker and thus prevents interdomain movement between the heme and Moco domain, which is believed to be crucial for intramolecular electron transfer between both domains (*50*). The finding that the apparent nitrate affinity is reduced suggests that 14-3-3 binding is strengthened for the nitrate-bound state of the enzyme. Such a mechanism would perfectly fit with the role of 14-3-3-mediated post-translational control of NR activity. The enzyme requires efficient inhibition when, for example, reducing equivalents are running short and consequently the product, toxic nitrite, might accumulate. Therefore, the nitrate-bound NR will be much more strongly inhibited. On the other hand, low nitrate concentrations might trigger 14-3-3 dissociation that in turn might increase the likelihood of phosphatases reversing the inhibitory circuit and thereby releasing again fully active NR.

ACKNOWLEDGMENT

We thank Nigel Crawford for providing plasmid pKK001 and Simona Jansen for excellent technical assistance.

SUPPORTING INFORMATION AVAILABLE

MALDI-TOF spectra (Figure 1) and deconvoluted Qtof MS/MS data of NR (Figure 2), CD spectroscopy results for the 14-3-3 proteins (Figure 3), and a sequence alignment of all 14-3-3 protein sequences according to The *Arabidopsis* Information Resource (www.tair.org) (Figure 4). This material is available free of charge via the Internet at http://pubs.acs.org.

REFERENCES

1. Miller, A. J., Fan, X., Orsel, M., Smith, S. J., and Wells, D. M. (2007) Nitrate transport and signalling. *J. Exp. Bot. 58*, 2297–2306.
2. Tsay, Y. F., Schroeder, J. I., Feldmann, K. A., and Crawford, N. M. (1993) The herbicide sensitivity gene CHL1 of *Arabidopsis* encodes a nitrate-inducible nitrate transporter. *Cell 72*, 705–713.
3. Lejay, L., Tillard, P., Lepetit, M., Olive, F., Filleur, S., Daniel-Vedele, F., and Gojon, A. (1999) Molecular and functional regulation of two NO_3^- uptake systems by N- and C-status of *Arabidopsis* plants. *Plant J. 18*, 509–519.
4. Dose, M. M., Hirasawa, M., Kleis-SanFrancisco, S., Lew, E. L., and Knaff, D. B. (1997) The ferredoxin-binding site of ferredoxin: Nitrite oxidoreductase. Differential chemical modification of the free enzyme and its complex with ferredoxin. *Plant Physiol. 114*, 1047–1053.
5. Campbell, W. H. (2001) Structure and function of eukaryotic NAD(P)H:nitrate reductase. *Cell. Mol. Life Sci. 58*, 194–204.
6. Fischer, K., Barbier, G. G., Hecht, H. J., Mendel, R. R., Campbell, W. H., and Schwarz, G. (2005) Structural basis of eukaryotic nitrate reduction: Crystal structures of the nitrate reductase active site. *Plant Cell 17*, 1167–1179.
7. Lu, G., Campbell, W. H., Schneider, G., and Lindqvist, Y. (1994) Crystal structure of the FAD-containing fragment of corn nitrate reductase at 2.5 Å resolution: Relationship to other flavoprotein reductases. *Structure 2*, 809–821.
8. Vincentz, M., and Caboche, M. (1991) Constitutive expression of nitrate reductase allows normal growth and development of *Nicotiana plumbaginifolia* plants. *EMBO J. 10*, 1027–1035.
9. Vincentz, M., Moureaux, T., Leydecker, M. T., Vaucheret, H., and Caboche, M. (1993) Regulation of nitrate and nitrite reductase

expression in *Nicotiana plumbaginifolia* leaves by nitrogen and carbon metabolites. *Plant J. 3*, 315–324.
10. Scheible, W. R., Gonzalez-Fontes, A., Lauerer, M., Muller-Rober, B., Caboche, M., and Stitt, M. (1997) Nitrate Acts as a Signal to Induce Organic Acid Metabolism and Repress Starch Metabolism in Tobacco. *Plant Cell 9*, 783–798.
11. Lillo, C. (2008) Signalling cascades integrating light-enhanced nitrate metabolism. *Biochem. J. 415*, 11–19.
12. Lillo, C., Meyer, C., Lea, U. S., Provan, F., and Oltedal, S. (2004) Mechanism and importance of post-translational regulation of nitrate reductase. *J. Exp. Bot. 55*, 1275–1282.
13. Lea, U. S., Leydecker, M. S., Quillere, I., Meyer, C., and Lillo, C. (2006) Posttranslational Regulation of Nitrate Reductase Strongly Affects the Levels of Free Amino Acids and Nitrate, whereas Transcriptional Regulation Has Only Minor Influence. *Plant Physiol. 140*, 1085–1094.
14. Glaab, J., and Kaiser, W. M. (1995) Inactivation of Nitrate Reductase involves NR-Protein Phosphorylation and Subsequent 'Binding' of an Inhibitor Protein. *Planta 4*, 514–518.
15. Kaiser, W. M., and Brendle-Behnisch, E. (1991) Rapid Modulation of Spinach Leaf Nitrate Reductase Activity by Photosynthesis: I. Modulation in Vivo by CO_2 Availability. *Plant Physiol. 96*, 363–367.
16. Huber, J. L., Huber, S. C., Campbell, W. H., and Redinbaugh, M. G. (1992) Reversible light/dark modulation of spinach leaf nitrate reductase activity involves protein phosphorylation. *Arch. Biochem. Biophys. 296*, 58–65.
17. MacKintosh, C. (1992) Regulation of spinach-leaf nitrate reductase by reversible phosphorylation. *Biochim. Biophys. Acta 1137*, 121–126.
18. Mackintosh, C., Douglas, P., and Lillo, C. (1995) Identification of a Protein That Inhibits the Phosphorylated Form of Nitrate Reductase from Spinach (*Spinacia oleracea*) Leaves. *Plant Physiol. 107*, 451–457.
19. Bachmann, M., McMichael, R. W., Jr., Huber, J. L., Kaiser, W. M., and Huber, S. C. (1995) Partial Purification and Characterization of a Calcium-Dependent Protein Kinase and an Inhibitor Protein Required for Inactivation of Spinach Leaf Nitrate Reductase. *Plant Physiol. 108*, 1083–1091.
20. Weiner, H., and Kaiser, W. M. (1999) 14-3-3 proteins control proteolysis of nitrate reductase in spinach leaves. *FEBS Lett. 455*, 75–78.
21. Cotelle, V., Meek, S. E., Provan, F., Milne, F. C., Morrice, N., and MacKintosh, C. (2000) 14-3-3s regulate global cleavage of their diverse binding partners in sugar-starved *Arabidopsis* cells. *EMBO J. 19*, 2869–2876.
22. Kaiser, W. M., and Huber, S. C. (2001) Post-translational regulation of nitrate reductase: Mechanism, physiological relevance and environmental triggers. *J. Exp. Bot. 52*, 1981–1989.
23. MacKintosh, C., and Meek, S. E. (2001) Regulation of plant NR activity by reversible phosphorylation, 14-3-3 proteins and proteolysis. *Cell. Mol. Life Sci. 58*, 205–214.
24. Provan, F., Aksland, L. M., Meyer, C., and Lillo, C. (2000) Deletion of the nitrate reductase N-terminal domain still allows binding of 14-3-3 proteins but affects their inhibitory properties. *Plant Physiol. 123*, 757–764.
25. Harthill, J. E., Meek, S. E., Morrice, N., Peggie, M. W., Borch, J., Wong, B. H., and Mackintosh, C. (2006) Phosphorylation and 14-3-3 binding of *Arabidopsis* trehalose-phosphate synthase 5 in response to 2-deoxyglucose. *Plant J. 47*, 211–223.
26. Nussaume, L., Vincentz, M., Meyer, C., Boutin, J. P., and Caboche, M. (1995) Post-transcriptional regulation of nitrate reductase by light is abolished by an N-terminal deletion. *Plant Cell 7*, 611–621.
27. Bachmann, M., Shiraishi, N., Campbell, W. H., Yoo, B. C., Harmon, A. C., and Huber, S. C. (1996) Identification of Ser-543 as the major regulatory phosphorylation site in spinach leaf nitrate reductase. *Plant Cell 8*, 505–517.
28. Douglas, P., Moorhead, G., Hong, Y., Morrice, N., and MacKintosh, C. (1998) Purification of a nitrate reductase kinase from *Spinacea oleracea* leaves, and its identification as a calmodulin-domain protein kinase. *Planta 206*, 435–442.
29. Sugden, C., Donaghy, P. G., Halford, N. G., and Hardie, D. G. (1999) Two SNF1-related protein kinases from spinach leaf phosphorylate and inactivate 3-hydroxy-3-methylglutaryl-coenzyme A reductase, nitrate reductase, and sucrose phosphate synthase in vitro. *Plant Physiol. 120*, 257–274.
30. Ikeda, Y., Koizumi, N., Kusano, T., and Sano, H. (2000) Specific binding of a 14-3-3 protein to autophosphorylated WPK4, an SNF1-related wheat protein kinase, and to WPK4-phosphorylated nitrate reductase. *J. Biol. Chem. 275*, 41528.
31. Baena-Gonzalez, E., Rolland, F., Thevelein, J. M., and Sheen, J. (2007) A central integrator of transcription networks in plant stress and energy signalling. *Nature 448*, 938–942.
32. Klimecka, M., and Muszynska, G. (2007) Structure and functions of plant calcium-dependent protein kinases. *Acta Biochim. Pol. 54*, 219–233.
33. Lee, J. Y., Yoo, B. C., and Harmon, A. C. (1998) Kinetic and calcium-binding properties of three calcium-dependent protein kinase isoenzymes from soybean. *Biochemistry 37*, 6801–6809.
34. Hernandez Sebastia, C., Hardin, S. C., Clouse, S. D., Kieber, J. J., and Huber, S. C. (2004) Identification of a new motif for CDPK phosphorylation in vitro that suggests ACC synthase may be a CDPK substrate. *Arch. Biochem. Biophys. 428*, 81–91.
35. Weekes, J., Ball, K. L., Caudwell, F. B., and Hardie, D. G. (1993) Specificity determinants for the AMP-activated protein kinase and its plant homologue analysed using synthetic peptides. *FEBS Lett. 334*, 335–339.
36. Halford, N. G., Hey, S., Jhurreea, D., Laurie, S., McKibbin, R. S., Paul, M., and Zhang, Y. (2003) Metabolic signalling and carbon partitioning: Role of Snf1-related (SnRK1) protein kinase. *J. Exp. Bot. 54*, 467–475.
37. Huber, S. C., and Huber, J. L. (1996) Role and Regulation of Sucrose-Phosphate Synthase in Higher Plants. *Annu. Rev. Plant Physiol. Plant Mol. Biol. 47*, 431–444.
38. Huang, J. Z., and Huber, S. C. (2001) Phosphorylation of synthetic peptides by a CDPK and plant SNF1-related protein kinase. Influence of proline and basic amino acid residues at selected positions. *Plant Cell Physiol. 42*, 1079–1087.
39. Rosenquist, M., Alsterfjord, M., Larsson, C., and Sommarin, M. (2001) Data mining the *Arabidopsis* genome reveals fifteen 14-3-3 genes. Expression is demonstrated for two out of five novel genes. *Plant Physiol. 127*, 142–149.
40. Gardino, A. K., Smerdon, S. J., and Yaffe, M. B. (2006) Structural determinants of 14-3-3 binding specificities and regulation of subcellular localization of 14-3-3-ligand complexes: A comparison of the X-ray crystal structures of all human 14-3-3 isoforms. *Semin. Cancer Biol. 16*, 173–182.
41. Bachmann, M., Huber, J. L., Liao, P. C., Gage, D. A., and Huber, S. C. (1996) The inhibitor protein of phosphorylated nitrate reductase from spinach (*Spinacia oleracea*) leaves is a 14-3-3 protein. *FEBS Lett. 387*, 127–131.
42. Kanamaru, K., Wang, R., Su, W., and Crawford, N. M. (1999) Ser-534 in the hinge 1 region of *Arabidopsis* nitrate reductase is conditionally required for binding of 14-3-3 proteins and in vitro inhibition. *J. Biol. Chem. 274*, 4160–4165.
43. Manak, M. S., and Ferl, R. J. (2007) Divalent cation effects on interactions between multiple *Arabidopsis* 14-3-3 isoforms and phosphopeptide targets. *Biochemistry 46*, 1055–1063.
44. Skipper, L., Campbell, W. H., Mertens, J. A., and Lowe, D. J. (2001) Pre-steady-state kinetic analysis of recombinant *Arabidopsis* NADH: nitrate reductase: Rate-limiting processes in catalysis. *J. Biol. Chem. 276*, 26995–27002.
45. Kuper, J., Llamas, A., Hecht, H. J., Mendel, R. R., and Schwarz, G. (2004) Structure of molybdopterin-bound Cnx1G domain links molybdenum and copper metabolism. *Nature 430*, 806–806.
46. Sehnke, P. C., Rosenquist, M., Alsterfjord, M., DeLille, J., Sommarin, M., Larsson, C., and Ferl, R. J. (2002) Evolution and isoform specificity of plant 14-3-3 proteins. *Plant Mol. Biol. 50*, 1011–1018.
47. Sehnke, P. C., DeLille, J. M., and Ferl, R. J. (2002) Consummating signal transduction: The role of 14-3-3 proteins in the completion of signal-induced transitions in protein activity. *Plant Cell 14* (Suppl.), S339–S354.
48. Sehnke, P. C., Laughner, B., Cardasis, H., Powell, D., and Ferl, R. J. (2006) Exposed loop domains of complexed 14-3-3 proteins contribute to structural diversity and functional specificity. *Plant Physiol. 140*, 647–660.
49. Moorhead, G., Douglas, P., Morrice, N., Scarabel, M., Aitken, A., and MacKintosh, C. (1996) Phosphorylated nitrate reductase from spinach leaves is inhibited by 14-3-3 proteins and activated by fusicoccin. *Curr. Biol. 6*, 1104–1113.
50. Barbier, G. G., and Campbell, W. H. (2005) Viscosity Effects on Eukaryotic Nitrate Reductase Activity. *J. Biol. Chem. 280*, 26049–26054.
51. Campbell, W. H. (1999) Nitrate reductase structure, function and regulation: Bridging the gap between biochemistry and physiology. *Annu. Rev. Plant Physiol. Plant Mol. Biol. 50*, 277–303.
52. Howard, W. D., and Solomonson, L. P. (1981) Kinetic mechanism of assimilatory NADH:nitrate reductase from *Chlorella*. *J. Biol. Chem. 256*, 12725–12730.
53. Barbier, G. G., Joshi, R. C., Campbell, E. R., and Campbell, W. H. (2004) Purification and biochemical characterization of simplified eukaryotic nitrate reductase expressed in *Pichia pastoris*. *Protein Expression Purif. 37*, 61–71.

54. Barber, M. J., Notton, B. A., Kay, C. J., and Solomonson, L. P. (1989) Chloride Inhibition of Spinach Nitrate Reductase. *Plant Physiol. 90*, 70–74.
55. Brody, M. S., and Hille, R. (1999) The kinetic behavior of chicken liver sulfite oxidase. *Biochemistry 38*, 6668–6677.
56. Jolly, S. O., Campbell, W., and Tolbert, N. E. (1976) NADPH- and NADH-nitrate reductases from soybean leaves. *Arch. Biochem. Biophys. 174*, 431–439.
57. Dwivedi, U. N., Shiraishi, N., and Campbell, W. H. (1994) Identification of an "essential" cysteine of nitrate reductase via mutagenesis of its recombinant cytochrome b reductase domain. *J. Biol. Chem. 269*, 13785–13791.
58. Athwal, G. S., and Huber, S. C. (2002) Divalent cations and polyamines bind to loop 8 of 14-3-3 proteins, modulating their interaction with phosphorylated nitrate reductase. *Plant J. 29*, 119–129.
59. Bachmann, M., Huber, J. L., Athwal, G. S., Wu, K., Ferl, R. J., and Huber, S. C. (1996) 14-3-3 proteins associate with the regulatory phosphorylation site of spinach leaf nitrate reductase in an isoform-specific manner and reduce dephosphorylation of Ser-543 by endogenous protein phosphatases. *FEBS Lett. 398*, 26–30.
60. Sehnke, P. C., Henry, R., Cline, K., and Ferl, R. J. (2000) Interaction of a plant 14-3-3 protein with the signal peptide of a thylakoid-targeted chloroplast precursor protein and the presence of 14-3-3 isoforms in the chloroplast stroma. *Plant Physiol. 122*, 235–242.
61. Chevalier, D., Morris, E. R., and Walker, J. C. (2009) 14-3-3 and FHA domains mediate phosphoprotein interactions. *Annu. Rev. Plant Biol. 60*, 67–91.
62. Chang, I. F., Curran, A., Woolsey, R., Quilici, D., Cushman, J. C., Mittler, R., Harmon, A., and Harper, J. F. (2009) Proteomic profiling of tandem affinity purified 14-3-3 protein complexes in *Arabidopsis thaliana*. *Proteomics 9*, 2967–2985.
63. Mehlmer, N., Wurzinger, B., Stael, S., Hofmann-Rodrigues, D., Csaszar, E., Pfister, B., Bayer, R., and Teige, M. (2010) The Ca^{2+}-dependent protein kinase CPK3 is required for MAPK-independent salt-stress acclimation in Arabidopsis. *Plant Journal 63*, 484–498.